

# Asteroid 2015 DB<sub>216</sub>: a recurring co-orbital companion to Uranus

C. de la Fuente Marcos<sup>\*</sup> and R. de la Fuente Marcos

*Apartado de Correos 3413, E-28080 Madrid, Spain*

Accepted 2015 July 27. Received 2015 July 7; in original form 2015 June 3

## ABSTRACT

Minor bodies trapped in 1:1 co-orbital resonances with a host planet could be relevant to explain the origin of captured satellites. Among the giant planets, Uranus has one of the smallest known populations of co-orbitals, three objects, and all of them are short-lived. Asteroid 2015 DB<sub>216</sub> has an orbital period that matches well that of Uranus, and here we investigate its dynamical state. Direct  $N$ -body calculations are used to assess the current status of this object, reconstruct its immediate dynamical past, and explore its future orbital evolution. A covariance matrix-based Monte Carlo scheme is presented and applied to study its short-term stability. We find that 2015 DB<sub>216</sub> is trapped in a temporary co-orbital resonance with Uranus, the fourth known minor body to do so. A detailed analysis of its dynamical evolution shows that it is an unstable but recurring co-orbital companion to Uranus. It currently follows an asymmetric horseshoe trajectory that will last for at least 10 kyr, but it may remain inside Uranus' co-orbital zone for millions of years. As in the case of other transient Uranian co-orbitals, complex multibody ephemeral mean motion resonances trigger the switching between the various resonant co-orbital states. The new Uranian co-orbital exhibits a secular behaviour markedly different from that of the other known Uranian co-orbitals because of its higher inclination, nearly 38°. Given its rather unusual discovery circumstances, the presence of 2015 DB<sub>216</sub> hints at the existence of a relatively large population of objects moving in similar orbits.

**Key words:** methods: numerical – methods: statistical – celestial mechanics – minor planets, asteroids: individual: 2015 DB<sub>216</sub> – planets and satellites: individual: Uranus.

## 1 INTRODUCTION

For over a century, co-orbitals —or minor bodies trapped in a 1:1 mean motion resonance with a host planet— have been regarded as mere interesting dynamical curiosities (Jackson 1913; Henon 1969; Namouni 1999). This view is now changing considerably; in fact, the heliocentric 1:1 co-orbital resonance could be an efficient mechanism for capture of satellites by a planet and therefore explain the origin of some irregular moons (Kortenkamp 2005). This theoretical possibility —that of being a feasible dynamical pathway to capture satellites, at least temporarily— was dramatically vindicated when a co-orbital of the Earth, 2006 RH<sub>120</sub>, remained as natural satellite of our planet for about a year starting in 2006 June (Kwiatkowski et al. 2009; Granvik, Vaubaillon & Jedicke 2012).

Uranus has one of the smallest known populations of co-orbitals and all of them are relatively short-lived (de la Fuente Marcos & de la Fuente Marcos 2014). So far, Uranus had only three known co-orbitals: 83982 Crantor (2002 GO<sub>9</sub>) (Gallardo 2006; de la Fuente Marcos & de la Fuente Marcos 2013), 2010 EU<sub>65</sub> (de la Fuente Marcos & de la Fuente Marcos 2013), and 2011 QF<sub>99</sub> (Alexandersen et al. 2013; de la Fuente Marcos & de la Fuente Marcos 2014). Due to its present short data-arc (85 d), 2010 EU<sub>65</sub>

is better described as a candidate. Asteroids Crantor and 2010 EU<sub>65</sub> follow horseshoe orbits, and 2011 QF<sub>99</sub> is an L<sub>4</sub> Trojan. Consistently, Uranus has also a small population of irregular satellites, significantly smaller than that of Jupiter or Saturn (Grav et al. 2003; Sheppard, Jewitt & Kleyna 2005). Most Uranian irregular satellites are retrograde and their large spread in semimajor axis suggest that they formed independently (Nesvorný et al. 2003); orbits with inclinations in the range (80°, 100°) are unstable due to the Kozai resonance (Kozai 1962). For the particular case of Uranus' Trojans, Dvorak, Bzszó & Zhou (2010) have also found that the stability depends on the orbital inclination and only the inclination intervals (0°, 7°), (9°, 13°), (31°, 36°), and (38°, 50°) seem to be stable. Asteroid 2011 QF<sub>99</sub> appears to inhabit one of these stable islands at an inclination of nearly 11° (de la Fuente Marcos & de la Fuente Marcos 2014). The stability of Uranian Trojans had been previously studied by Marzari, Tricarico & Scholl (2003), and by Nesvorný & Dones (2002) and Holman & Wisdom (1993) before them.

Here, we present a recently discovered object, 2015 DB<sub>216</sub>, that is also trapped in a 1:1 mean motion resonance with Uranus. This minor body exhibits some dynamical features that separate it from the previously known Uranian co-orbitals. This paper is organized as follows. In Section 2, we briefly discuss both the data and the numerical model used in our calculations. The topic of generating control orbits compatible with the available observations and

\* E-mail: carlosdlfmarcos@gmail.com

**Table 1.** Heliocentric Keplerian orbital elements of 2015 DB<sub>216</sub> used in this research. The orbit is based on 28 observations spanning a data-arc of 4200 days or 11.50 yr, from 2003 October 21 to 2015 April 23. Values include the  $1\sigma$  uncertainty. The orbit is computed at epoch JD 2457000.5 that corresponds to 0:00 UT on 2014 December 9 (J2000.0 ecliptic and equinox) and it is  $t = 0$  in the figures. Source: JPL Small-Body Database.

Semimajor axis, $a$ (au)	=	19.204±0.005
Eccentricity, $e$	=	0.32395±0.00013
Inclination, $i$ (°)	=	37.7173±0.0003
Longitude of the ascending node, $\Omega$ (°)	=	6.2679±0.0003
Argument of perihelion, $\omega$ (°)	=	237.75±0.03
Mean anomaly, $M$ (°)	=	302.52±0.04
Perihelion, $q$ (au)	=	12.9832±0.0013
Aphelion, $Q$ (au)	=	25.426±0.007
Absolute magnitude, $H$ (mag)	=	8.3±0.4

its implications is considered in Section 3. The current status of 2015 DB<sub>216</sub> is studied in Section 4, where its dynamical past and future orbital evolution are also investigated. Section 5 discusses our results and their possible significance. The stability of the co-orbital realm located in the neighbourhood of 2015 DB<sub>216</sub> is tentatively explored in Section 6. A summary of our conclusions is given in Section 7.

## 2 DATA AND METHODOLOGY

Asteroid 2015 DB<sub>216</sub> was discovered on 2015 February 27 at Mt. Lemmon Survey. With a value of the semimajor axis  $a = 19.20$  au, this Centaur moves in an eccentric,  $e = 0.32$ , and highly inclined path,  $i = 37^\circ 72'$ . With such an orbit, close encounters are only possible with Uranus as its perihelion is well beyond Saturn's aphelion and its aphelion far from Neptune's perihelion. It is a relatively large object with  $H = 8.3$  mag which translates into a diameter in the range 46–145 km for an assumed albedo of 0.40–0.04. Its period of revolution around the Sun, approximately 84.16 yr at present, is very close to that of Uranus which is suggestive of an object that moves co-orbital with the giant planet. Its current orbit is statistically robust because six precovery images acquired by the Sloan Digital Sky Survey (SDSS) at Apache Point late in 2003 have been found. The heliocentric Keplerian osculating orbital elements and uncertainties in Table 1 are based on 28 observations for a data-arc span of 4200 d and they have been obtained from the Jet Propulsion Laboratory (JPL) Small-Body Database.<sup>1</sup>

In order to assess the dynamical status of 2015 DB<sub>216</sub>, we use the Hermite integration scheme described by Makino (1991) and implemented by Aarseth (2003). The standard version of this direct  $N$ -body code is publicly available from the IoA web site.<sup>2</sup> Our physical model includes the perturbations by the eight major planets, the Moon, the barycentre of the Pluto–Charon system, and the three largest asteroids; additional details can be found in de la Fuente Marcos & de la Fuente Marcos (2012). To compute accurate initial positions and velocities we used the heliocentric ecliptic Keplerian elements provided by the JPL On-line Solar System Data Service<sup>3</sup> (Giorgini et al. 1996) and initial positions and velocities based on the DE405 planetary orbital ephemerides (Standish 1998)

referred to the barycentre of the Solar system. Besides the orbital calculations completed using the nominal elements in Table 1, we have performed 50 control simulations with sets of orbital elements obtained from the nominal ones as described in the following section, all of them for 0.5 Myr forward and backwards in time. Two more sets of 100 control orbits each have been integrated for just 5 kyr into the past and the future to better characterize its short-term stability.

## 3 GENERATING CONTROL ORBITS WITH MONTE CARLO AND THE COVARIANCE MATRIX

For a given minor body, the orbital elements are a coordinate in six-dimensional space (assuming as we do that non-gravitational forces can be neglected), which represents the location where samples of control orbits are most likely to be generated. This is analogous to the peak of the Gaussian curve for a typical one-dimensional or univariate normal distribution. The multivariate normal distribution is a generalization of the one-dimensional normal distribution to higher dimensions. Instead of being specified by its mean value and variance, such a distribution is characterized by its mean (a vector with the mean of the multidimensional distribution) and covariance matrix, which defines an hyperellipsoid in multidimensional space. The values of the elements of the covariance matrix indicate the level to which two given variables vary together. For a particular object, both mean and covariance matrix are computed from the observations.

When studying the stability of the orbital solution of a certain minor planet, we can compute the orbital elements of the control orbits varying them randomly, within the ranges defined by their mean values and standard deviations. For example, a new value of the orbital eccentricity can be found using the expression  $e_c = e + \sigma_e r_1$ , where  $e_c$  is the eccentricity of the control orbit,  $e$  is the mean value of the eccentricity (nominal orbit),  $\sigma_e$  is the standard deviation of  $e$  (nominal orbit), and  $r_1$  is a (pseudo) random number with normal distribution in the range  $-1$  to  $1$ . In statistical terms, the univariate Gaussian distribution results from adding a standard Gaussian variate with mean zero and variance one multiplied by the standard deviation, to the mean value. This is equivalent to considering a number of different virtual minor planets moving in similar orbits, not a sample of control orbits incarnated from a set of observations obtained for a single minor planet. If the control orbits are meant to be compatible with actual observations, we have to consider how the elements affect each other using the covariance matrix or e.g. following the procedure described in Sitarski (1998, 1999, 2006).

The methodology used in this paper is an implementation of the classical Monte Carlo using the Covariance Matrix (MCCM, Bordovitsyna, Avdyushev & Chernitsov 2001; Avdyushev & Banchikova 2007) approach, i.e. a Monte Carlo process creates control orbits with initial parameters from the nominal orbit adding random noise on each initial orbital element making use of the covariance matrix. The MCCM approach considers that the estimated parameters are Gaussian random variables with mean values those of the nominal orbit and covariance matrix obtained via the least-squares method applied to the available observations. Assuming a covariance matrix as computed by the JPL Solar System Dynamics Group, Horizons On-Line Ephemeris System, the vector including the mean values of the orbital parameters at a given epoch  $t_0$  is of the form  $\mathbf{v} = (e, q, \tau, \Omega, \omega, i)$ ; the perihelion is given by the expression  $q = a(1 - e)$ . If  $\mathbf{C}$  is the covariance matrix at the same epoch

<sup>1</sup> <http://ssd.jpl.nasa.gov/sbdb.cgi>

<sup>2</sup> <http://www.ast.cam.ac.uk/~sverre/web/pages/nbody.htm>

<sup>3</sup> [http://ssd.jpl.nasa.gov/?planet\\_pos](http://ssd.jpl.nasa.gov/?planet_pos)

associated with the nominal orbital solution that is symmetric and positive-semidefinite, then  $\mathbf{C} = \mathbf{A} \mathbf{A}^T$ , where  $\mathbf{A}$  is a lower triangular matrix with real and positive diagonal elements,  $\mathbf{A}^T$  is the transpose of  $\mathbf{A}$ . In the particular case studied here, these matrices are  $6 \times 6$ . If the elements of  $\mathbf{C}$  are written as  $c_{ij}$  and those of  $\mathbf{A}$  as  $a_{ij}$ , where those are the entries in the  $i$ -th row and  $j$ -th column, they are related by the following expressions:

$$\begin{aligned}
a_{11} &= \sqrt{c_{11}} \\
a_{21} &= c_{12}/a_{11} \\
a_{31} &= c_{13}/a_{11} \\
a_{41} &= c_{14}/a_{11} \\
a_{51} &= c_{15}/a_{11} \\
a_{61} &= c_{16}/a_{11} \\
a_{22} &= \sqrt{c_{22} - a_{21}^2} \\
a_{32} &= (c_{23} - a_{21} a_{31})/a_{22} \\
a_{42} &= (c_{24} - a_{21} a_{41})/a_{22} \\
a_{52} &= (c_{25} - a_{21} a_{51})/a_{22} \\
a_{62} &= (c_{26} - a_{21} a_{61})/a_{22} \\
a_{33} &= \sqrt{c_{33} - a_{31}^2 - a_{32}^2} \\
a_{43} &= (c_{34} - a_{31} a_{41} - a_{32} a_{42})/a_{33} \\
a_{53} &= (c_{35} - a_{31} a_{51} - a_{32} a_{52})/a_{33} \\
a_{63} &= (c_{36} - a_{31} a_{61} - a_{32} a_{62})/a_{33} \\
a_{44} &= \sqrt{c_{44} - a_{41}^2 - a_{42}^2 - a_{43}^2} \\
a_{54} &= (c_{45} - a_{41} a_{51} - a_{42} a_{52} - a_{43} a_{53})/a_{44} \\
a_{64} &= (c_{46} - a_{41} a_{61} - a_{42} a_{62} - a_{43} a_{63})/a_{44} \\
a_{55} &= \sqrt{c_{55} - a_{51}^2 - a_{52}^2 - a_{53}^2 - a_{54}^2} \\
a_{65} &= (c_{56} - a_{51} a_{61} - a_{52} a_{62} - a_{53} a_{63} - a_{54} a_{64})/a_{55} \\
a_{66} &= \sqrt{c_{66} - a_{61}^2 - a_{62}^2 - a_{63}^2 - a_{64}^2 - a_{65}^2}.
\end{aligned} \tag{1}$$

If  $\mathbf{r}$  is a vector made of univariate Gaussian random numbers (components  $r_i$  with  $i = 1, 6$ ), the required multivariate Gaussian random samples —i.e. the sets of initial orbital elements of the control orbits— are given by the expressions (assuming the structure provided by the JPL Horizons On-Line Ephemeris System),  $\mathbf{v}_c = \mathbf{v} + \mathbf{A} \mathbf{r}$ :

$$\begin{aligned}
e_c &= e + a_{11} r_1 \\
q_c &= q + a_{22} r_2 + a_{21} r_1 \\
\tau_c &= \tau + a_{33} r_3 + a_{32} r_2 + a_{31} r_1 \\
\Omega_c &= \Omega + a_{44} r_4 + a_{43} r_3 + a_{42} r_2 + a_{41} r_1 \\
\omega_c &= \omega + a_{55} r_5 + a_{54} r_4 + a_{53} r_3 + a_{52} r_2 + a_{51} r_1 \\
i_c &= i + a_{66} r_6 + a_{65} r_5 + a_{64} r_4 + a_{63} r_3 + a_{62} r_2 + a_{61} r_1.
\end{aligned} \tag{2}$$

In contrast, the equivalent classical—but statistically wrong—expressions commonly used to generate control orbits are given by:

$$\begin{aligned}
e_c &= e + \sigma_e r_1 \\
q_c &= q + \sigma_q r_2 \\
\tau_c &= \tau + \sigma_\tau r_3 \\
\Omega_c &= \Omega + \sigma_\Omega r_4 \\
\omega_c &= \omega + \sigma_\omega r_5 \\
i_c &= i + \sigma_i r_6.
\end{aligned} \tag{3}$$

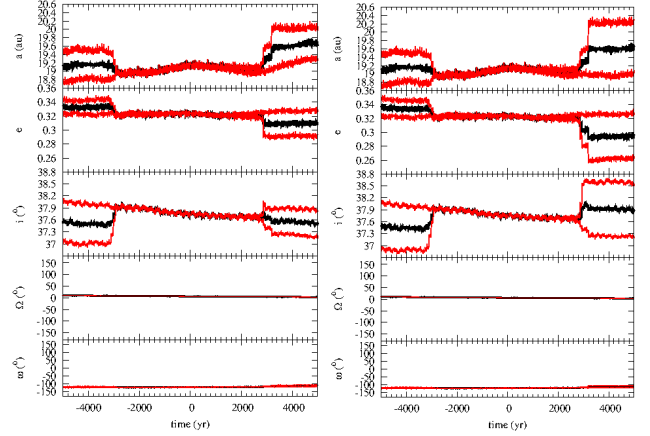


**Figure 1.** Time evolution of the orbital elements  $a$ ,  $e$ ,  $i$ ,  $\Omega$ , and  $\omega$  of 2015 DB<sub>216</sub>. The thick black curve shows the average evolution of 100 control orbits, the thin red curves display the ranges in the values of the parameters at the given time. Control orbits depicted in the left-hand panels have been computed as described in the text, using the covariance matrix (Eqs. 2). Those displayed in the right-hand panels have been computed without taking into account the covariance matrix (Eqs. 3).

A comparison between the results of the evolution of a sample of control orbits generated using Eqs. 2 and 3 for the particular case of 2015 DB<sub>216</sub> appears in Fig. 1, left-hand and right-hand panels, respectively. In our calculations, the Box-Muller method (Press et al. 2007) was used to generate random numbers with a normal distribution. It is obvious that, at least for this particular object, the difference is not very significant. However and for very precise orbits, the outcomes from these two approaches could be very different (see e.g. fig. 5 in Sitarski 1998); creating control orbits by randomly varying the nominal orbital elements in range of their mean errors (Eqs. 3) is not recommended in that case.

#### 4 ASTEROID 2015 DB<sub>216</sub>: DYNAMICAL EVOLUTION

In order to assess the dynamical status of 2015 DB<sub>216</sub>, we focus on the study of the librational behaviour of the relative mean longitude  $\lambda_r = \lambda - \lambda_U$ , where  $\lambda$  and  $\lambda_U$  are the mean longitudes of the object and Uranus, respectively;  $\lambda = M + \Omega + \omega$ , where  $M$  is the mean anomaly,  $\Omega$  is the longitude of the ascending node, and  $\omega$  is the argument of perihelion. If  $\lambda_r$  oscillates around  $0^\circ$ , the object is considered a quasi-satellite; Trojan bodies are characterized by  $\lambda_r$  librating around  $+60^\circ$  (L<sub>4</sub> Trojan) or  $-60^\circ$  (or  $300^\circ$ , L<sub>5</sub> Trojan); finally, an object whose  $\lambda_r$  oscillates with amplitude  $> 180^\circ$  follows a horseshoe orbit (see e.g. Murray & Dermott 1999). Quasi-satellites are not true gravitationally bound satellites but appear to orbit the host planet like a retrograde satellite. If  $\lambda_r$  can take any value (circulates), we speak of passing orbits.

Our  $N$ -body integrations show that 2015 DB<sub>216</sub> is currently a co-orbital companion to Uranus and moves in an asymmetric horseshoe orbit with a period of about 11 kyr (see Fig. 2, right-hand panel); in this case, asymmetric means that the resonant angle,  $\lambda_r$ , goes beyond  $0^\circ$  reaching an offset of libration around  $-40^\circ$  at nearly 9 kyr. The left-hand panel in Fig. 2 depicts the trajectory of 2015 DB<sub>216</sub> viewed in a frame of reference corotating with Uranus. Figure 3 displays the dynamical evolution of various parameters for three representative orbits: the nominal one (central panels) and those of two additional orbits which are most different from the

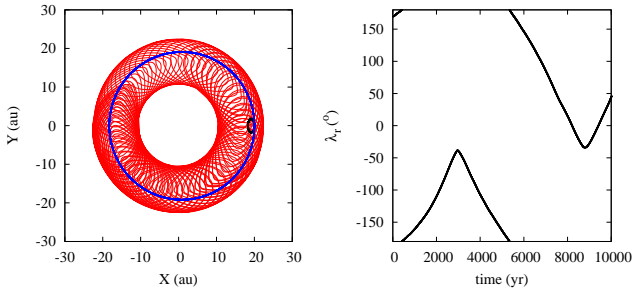


**Figure 2.** The motion of 2015 DB<sub>216</sub> during the time interval (0, 10) kyr projected on to the ecliptic plane in a coordinate system rotating with Uranus (red curve, left-hand panel). The orbit and the position of Uranus are also plotted (blue curve). In this frame of reference, and as a result of its non-negligible eccentricity, Uranus describes a small ellipse (black curve). The associated values of the resonant angle,  $\lambda_r$ , are also displayed (right-hand panel).

previous one, and have been obtained adding (+) or subtracting (−) 6-times the uncertainty from the orbital parameters (the six elements) in Table 1. All the control orbits show consistent behaviour within a few thousand years of  $t = 0$  (see Fig. 1). Its  $e$ -folding time, or characteristic time-scale on which two arbitrarily close orbits diverge exponentially, is a few thousand years both in the past and the future. The evolution of the control orbits exhibits very similar behaviour of all the orbital elements within the time frame (−3, 3) kyr (see Fig. 1).

Asteroid 2015 DB<sub>216</sub> currently occupies (see Fig. 3, E-panels) a band of instability between the two stable islands in inclination, (31°, 36°) and (38°, 50°), described in Dvorak et al. (2010) for Uranian Trojans. However, the figure shows that the inclination of this asteroid is high enough to avoid close encounters with Uranus when the relative mean longitude approaches zero i.e. close encounters with Uranus (or any other body) are not responsible for the activation and deactivation of the co-orbital behaviour of this object. Very few close encounters with Uranus have been observed during the simulated time (examples appear in the A-left-hand and central panels of Fig. 3). However, multiple and repetitive short co-orbital episodes of the Trojan, quasi-satellite and horseshoe type are observed in Fig. 3. Recurrent co-orbital episodes in which the relative mean longitude librates for several cycles and then circulates for a few more cycles before restarting libration once again, are the signpost of a type of dynamical behaviour known as resonance angle nodding, see e.g. Ketchum, Adams & Bloch (2013); nodding often occurs when a small body is in an external (near) mean motion resonance with a larger planet. In our case, the situation is more complicated because we have multiple distant perturbers.

Transitions in and out or between the various co-orbital states are not triggered by encounters but result from complex multi-body ephemeral mean motion resonances as described in de la Fuente Marcos & de la Fuente Marcos (2014). As other Uranian co-orbitals do, 2015 DB<sub>216</sub> moves in near resonance with the other three giant planets: 1:7 with Jupiter, 7:20 with Saturn, and 2:1 with Neptune. Figure 4 shows the behaviour of the resonant arguments  $\sigma_J = 7\lambda - \lambda_J - 6\varpi$ ,  $\sigma_S = 20\lambda - 7\lambda_S - 13\varpi$ , and  $\sigma_N = \lambda - 2\lambda_N + \varpi$ , where  $\lambda_J$  is the mean longitude of Jupiter,  $\lambda_S$  is the mean longitude of Saturn,  $\lambda_N$  is the mean longitude of Neptune, and  $\varpi = \Omega + \omega$  is the longitude of the perihelion of 2015 DB<sub>216</sub>. The plot (similar to figs. 6 and 7 in de la Fuente Marcos & de la Fuente Marcos 2014) clearly indicates that transitions are quickly triggered when multiple mean motion resonances work in unison. In Fig. 4, an

originally passing orbit becomes a horseshoe path after  $\sigma_J$  and  $\sigma_N$  stop circulating; prior to the ejection from the horseshoe-like path, the same scenario is observed. The dynamical role of three-body mean motion resonances has been recently explored by Gallardo (2014). Marzari et al. (2003) already pointed out that three-body resonances could be a source of instability for Uranian co-orbitals, in particular Trojans.

It may be argued that it is unclear from Fig. 4 that overlapping mean motion resonances are responsible for the transitions between co-orbital states or the activation/deactivation of the observed librational dynamics. On strictly theoretical grounds, this is to be expected as the orbital architecture of the giant planets is not random. Ito & Tanikawa (2002) and Tanikawa & Ito (2007) have pointed out that Jupiter affects the motions of Uranus and Neptune without the connection of Saturn and that secular perturbations may be nullified in such context. To explore this issue further, we have recomputed the short-term orbital evolution of the nominal orbit of 2015 DB<sub>216</sub> using increasingly complex physical models. Integrating the three-body problem—Sun, Uranus, and 2015 DB<sub>216</sub>—we observe asymmetric horseshoe evolution with no transitions. Computing the evolution of the four-body problem—Sun, Jupiter, Uranus, and 2015 DB<sub>216</sub>—a transition from asymmetric horseshoe to L<sub>4</sub> Trojan at about 15 kyr is recorded. The alternative four-body problem—Sun, Saturn, Uranus, and 2015 DB<sub>216</sub>—results in an L<sub>4</sub> Trojan path with no transitions. A similar result is observed for the case Sun, Uranus, Neptune, and 2015 DB<sub>216</sub>. The six-body problem—Sun, Jupiter, Saturn, Uranus, Neptune, and 2015 DB<sub>216</sub>—results in an asymmetric horseshoe transitioning to a passing orbit, but somewhat earlier than observed in Fig. 4. It appears obvious that in order to turn the asymmetric horseshoe libration into a passing orbit, superposition of mean motion resonances is required.

A more systematic exploration of the various five-, six- and higher-multiplicity-body problems shows that the details of the transitions are strongly dependent on the number of distant perturbers included in the simulations. The dynamical evolution of these objects is unusually sensitive to the physical model used to perform the calculations. Removing the three asteroids and the Pluto-Charon system does not have a major observable impact on the outcome of the simulations both in terms of the timing and the types of the observed transitions (the evolution displayed in Fig. 4 remains very nearly the same). However, stripping planets from the model—even Mercury or Mars—has immediate effects on the orbital evolution of these recurring Uranian co-orbitals. For example, removing Mercury from the calculations triggers a transition from asymmetric horseshoe to L<sub>4</sub> Trojan at about 15 kyr and back to asymmetric horseshoe a few kyr later. This analysis indicates that any numerical study of these objects that is not using the full set of planets may arrive to unrealistic conclusions regarding the stability and dynamical evolution of these objects. This is consistent with the analysis in Tanikawa & Ito (2007). Published works like those of Marzari et al. (2003) or Alexandersen et al. (2013) made use of a five-body model including the Sun and the four outer planets.

As for the secular behaviour (see Fig. 5), it is markedly different from the one described for other Uranian co-orbitals in de la Fuente Marcos & de la Fuente Marcos (2014). The precession frequency of the longitude of the perihelion of 2015 DB<sub>216</sub>,  $\varpi = \Omega + \omega$ , is only in secular resonance with Neptune and for a limited time. The value of  $\Delta\varpi = \varpi - \varpi_N$  librates around 180°. The absence of apsidal corotation resonances (see Lee & Peale 2002; Beaugé, Ferraz-Mello & Michtchenko 2003) probably translates into increased stability of this object when compared with other Uranian co-orbitals. Even if evidently chaotic, its dynamical evolu-

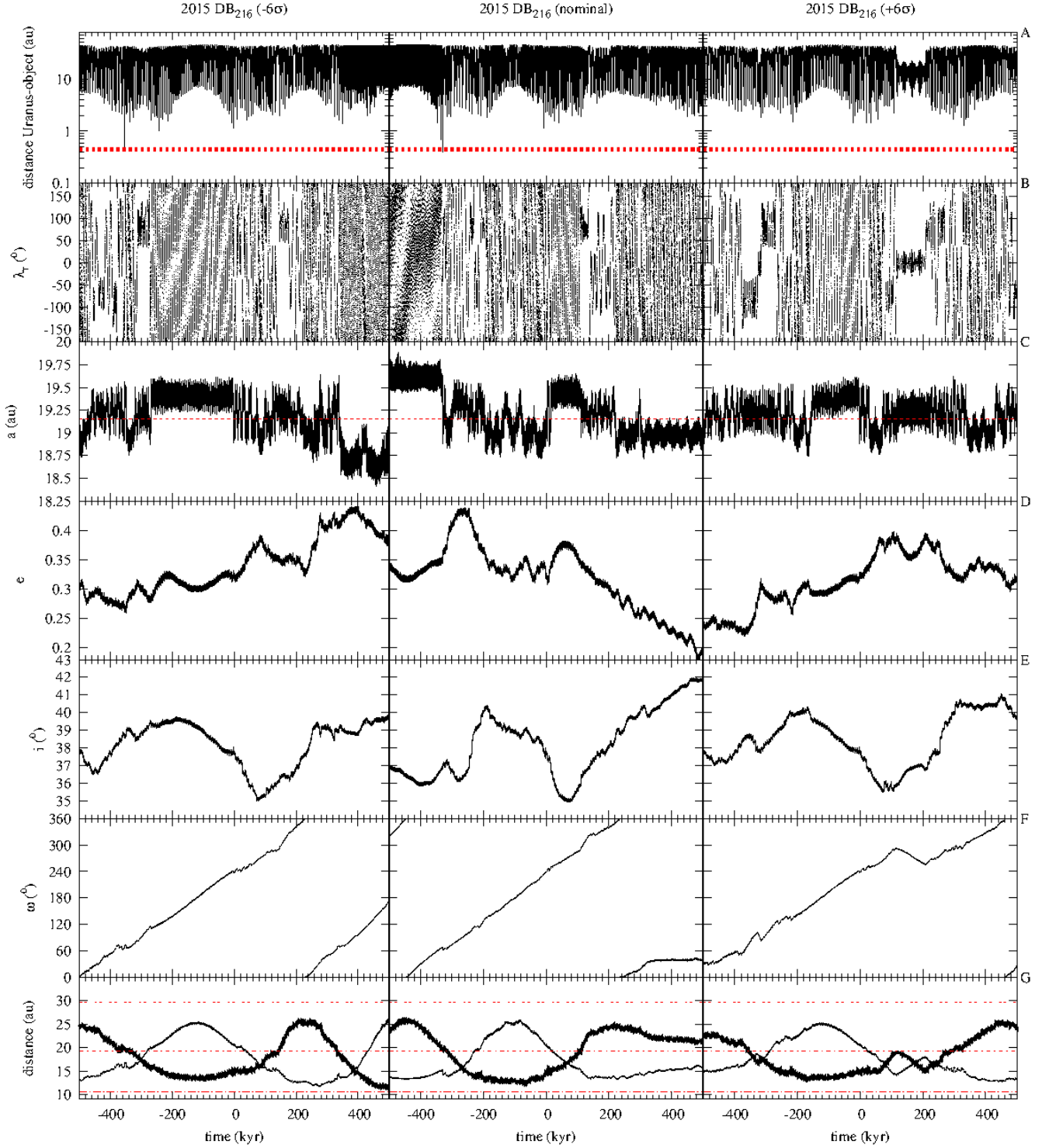


**Figure 3.** Comparative dynamical evolution of various parameters for the nominal orbit of 2015 DB<sub>216</sub> as presented in Table 1 (central panels) and two representative orbits that are most different from the nominal one (see the text for details). The distance from Uranus (A-panels); the value of the Hill sphere radius of Uranus, 0.4469 au, is displayed as a red line. The resonant angle,  $\lambda_r$  (B-panels). The orbital elements  $a$  (C-panels, the value of the semimajor axis of Uranus appears as a red line),  $e$  (D-panels),  $i$  (E-panels) and  $\omega$  (F-panels). The distances to the descending (thick line) and ascending nodes (dotted line) appear in the G-panels. Saturn and Neptune ap/peri distances are also shown as red lines.

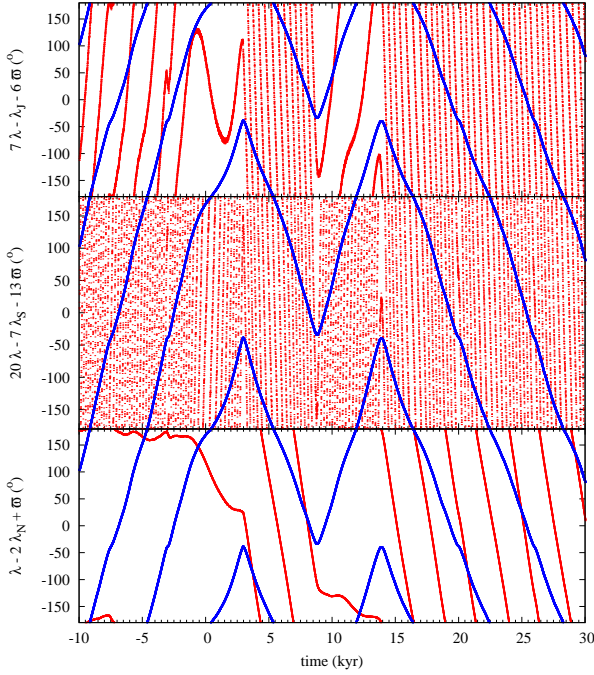


**Figure 4.** Resonant arguments  $\sigma_J = 7\lambda - \lambda_J - 6\varpi$  (top panel),  $\sigma_S = 20\lambda - 7\lambda_S - 13\varpi$  (middle panel), and  $\sigma_N = \lambda - 2\lambda_N + \varpi$  (bottom panel) plotted against time for the time interval  $(-10, 30)$  kyr. The relative mean longitude with respect to Uranus appears as a thick blue line. The angle  $\sigma_S$  alternates between circulation and asymmetric libration, indicating that the motion is chaotic. The observed resonant evolution is consistent across control orbits.

tion appears to be relatively stable and the object may remain in the neighbourhood of Uranus co-orbital region for millions of years. On the other hand, during the quasi-satellite episode observed in Fig. 3, right-hand panels, the object exhibits Kozai-like dynamics with  $\omega$  librating around  $270^\circ$  for about 100 kyr.

## 5 DISCUSSION

Our analysis suggests that, even if submitted to chaotic dynamics, this object may be intrinsically more stable than any of the previously known Uranian co-orbitals, but there is an additional piece of robust evidence in favour of this interpretation. Asteroid 2015 DB<sub>216</sub> was serendipitously discovered by a survey aimed at finding near-Earth objects (NEOs), the Mt. Lemmon Survey (MLS), that is part of the Catalina Sky Survey (CSS)<sup>4</sup> and precovered from observations acquired by the SDSS,<sup>5</sup> a project aimed at creating the most detailed three-dimensional maps of the Universe ever made after imaging about one-third of the sky. Therefore, its observation (past and present) was not the result of careful planning like it was the case of the discovery of 2011 QF<sub>99</sub> (Alexandersen et al. 2013). In de la Fuente Marcos & de la Fuente Marcos (2014), section 8, we studied the discovery circumstances of known Uranian co-orbitals and candidates. All of them have been found at declinations in the range  $-2^\circ$  to  $+15^\circ$  (see Table 2). In sharp contrast, 2015 DB<sub>216</sub> was observed at declination  $+57.3^\circ$  by SDSS in

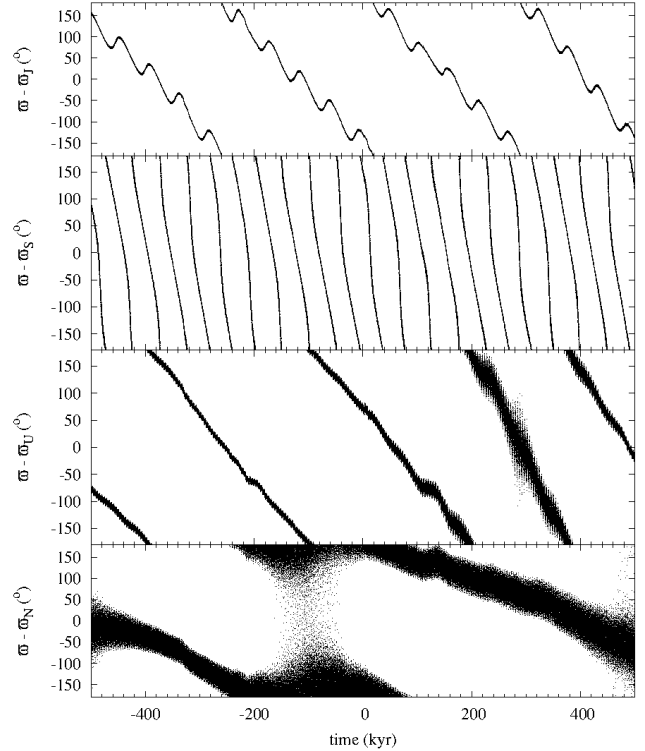


**Figure 5.** Time evolution of the relative longitude of the perihelion,  $\Delta\varpi$ , of 2015 DB<sub>216</sub> with respect to the giant planets: referred to Jupiter ( $\varpi - \varpi_J$ ), to Saturn ( $\varpi - \varpi_S$ ), to Uranus ( $\varpi - \varpi_U$ ), and to Neptune ( $\varpi - \varpi_N$ ). The relative longitudes circulate over the entire simulated period with the exception of that of Neptune. These results are for the nominal orbit in Table 1.

2003 and at  $+29.5^\circ$  by MLS in 2015. In de la Fuente Marcos & de la Fuente Marcos (2014), fig. 18, an observational bias regarding the observation of Uranian co-orbitals was pointed out, that co-orbitals reaching perigee (or perihelion) near declination  $0^\circ$  are nearly six times more likely to be found than those reaching perigee at declinations  $\pm 60^\circ$ , if they do exist.

Table 2 includes data from the Minor Planet Center (MPC) Database<sup>6</sup> and clearly shows that, among Uranian co-orbitals, 2015 DB<sub>216</sub> is a puzzling outlier. Assuming that this object is not a statistical accident, its presence hints at the existence of a significant population of objects moving in similar orbits, perhaps an order of magnitude larger than current models predict for regular Uranian co-orbitals. The absence of secular perturbations by Jupiter and Uranus found for 2015 DB<sub>216</sub> may probably explain the relative stability of this putative population. It could be the case that —after all— Uranus may host a large population of (transient but recurring) co-orbitals, but their orbits may be characterized by high orbital inclinations. The discovery of 2015 DB<sub>216</sub> parallels that of 83982 Crantor (2002 GO<sub>9</sub>), found by the Near-Earth Asteroid Tracking (NEAT) project at Palomar Observatory in 2002 and precovered from images obtained in 2001 by the Air Force Maui Optical and Supercomputing (AMOS) observatory and SDSS.

<sup>4</sup> [http://www.lpl.arizona.edu/css/css\\_facilities.html](http://www.lpl.arizona.edu/css/css_facilities.html)

<sup>5</sup> <http://www.sdss.org>

<sup>6</sup> [http://www.minorplanetcenter.net/db\\_search](http://www.minorplanetcenter.net/db_search)

**Table 2.** Equatorial coordinates and apparent magnitudes (with filter) at discovery time of known Uranian co-orbitals and candidates (J2000.0 ecliptic and equinox). Source: MPC Database.

Object	$\alpha$ (h:m:s)	$\delta$ (°:′:″)	$m$ (mag)
1999 HD <sub>12</sub>	12:31:54.80	-01:03:07.9	22.9 (R)
(83982) Crantor	14:10:43.80	+01:24:45.5	19.2 (R)
2002 VG <sub>131</sub>	00:54:57.98	+12:07:52.4	22.5 (R)
2010 EU <sub>65</sub>	12:15:58.608	-02:07:16.66	21.2 (R)
2011 QF <sub>99</sub>	01:57:34.729	+14:35:44.64	22.8 (r)
2015 DB <sub>216</sub> (SDSS, 2003)	08:29:42.21	+57:19:08.2	22.4 (V)
2015 DB <sub>216</sub> (MLS, 2015)	11:09:56.70	+29:31:01.6	20.5 (V)

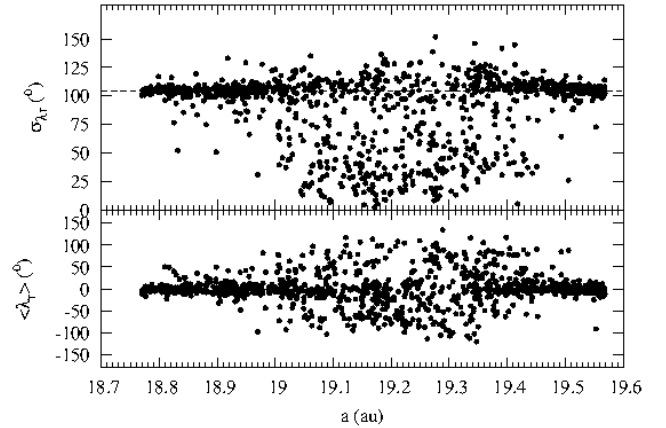
## 6 EXPLORING THE ORBITAL DOMAIN NEAR 2015 DB<sub>216</sub>

It could be debated that arguing on the existence of a population of high orbital inclination Uranian co-orbitals based solely on the discovery of 2015 DB<sub>216</sub> is an exercise of mere speculation. In order to investigate this interesting hypothesis further, we have studied the evolution of a sample of  $10^3$  fictitious bodies with initial orbits similar to that of 2015 DB<sub>216</sub>. Their orbital elements have been generated using uniformly distributed random numbers in order to survey the relevant region of the orbital parameter space evenly. For each test orbit, a numerical integration for  $10^4$  yr—using the same physical model and techniques applied in previous sections—has been performed.

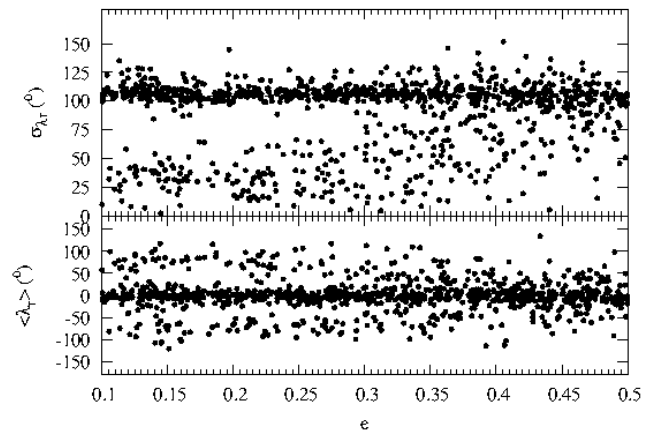
The average value (bottom panels) of the resonant angle,  $\lambda_r$ , and its standard deviation (top panels) as a function of the initial values of the orbital parameters  $a$ ,  $e$  and  $i$  is plotted in Figs 6–8, respectively. The assumed ranges in  $a$ ,  $e$  and  $i$  are displayed;  $\Omega$  and  $\omega$  are chosen in the range  $0^\circ$ – $360^\circ$ . An object following a strict passing orbit has an average value of the resonant angle close to  $0^\circ$  and its associated standard deviation is nearly  $104^\circ$  (also displayed on the top panel of the figures as a dashed line); the value of the variance of a continuous uniform distribution of maximum value  $x_{\max}$  and minimum value  $x_{\min}$  is given by the expression  $(x_{\max} - x_{\min})^2/12$ , and the mean value is  $(x_{\max} + x_{\min})/2$ . Consistently with our analysis of the dynamics of 2015 DB<sub>216</sub> in which recurring co-orbital episodes of various types are observed, the fictitious orbits studied here show values of the standard deviation of the resonant angle in obvious conflict with those expected in a non-librational scenario. Therefore, there is a robust theoretical ground to assume that such population of high orbital inclination Uranian recurring co-orbitals may exist.

Figure 8 shows that the initial value of the orbital inclination does not have a major impact on  $\langle \lambda_r \rangle$  or  $\sigma_{\lambda_r}$  (for the ranges of the values of the orbital elements considered here), but Fig. 7 indicates that the initial value of the orbital eccentricity has a major influence on the subsequent evolution of the test orbit. For values in the range 0.1–0.3 the magnitude of the standard deviation of the resonant angle tends to be significantly lower when recurring co-orbital behaviour appears. These orbits are inherently more stable as their perihelia and aphelia are less directly perturbed. They are associated with Trojan and quasi-satellite co-orbital states.

Returning to the issue of the actual extension of the Uranian co-orbital zone for these high-inclination, transient but recurring co-orbitals, the distribution in semimajor axis (the initial value) for test orbits with  $\sigma_{\lambda_r} \in (100^\circ, 108^\circ)$  (top panel) and outside that range (bottom panel) is plotted in Fig. 9. The distribution clearly



**Figure 6.** Mean value (bottom panel) and standard deviation (top panel) of the resonant angle,  $\lambda_r$ , as a function of the initial value of the semimajor axis. The value of the standard deviation for a continuous uniform distribution of maximum value  $180^\circ$  and minimum value  $-180^\circ$  is also indicated,  $\sim 104^\circ$ .



**Figure 7.** Same as Fig. 6 but for the initial value of the eccentricity.

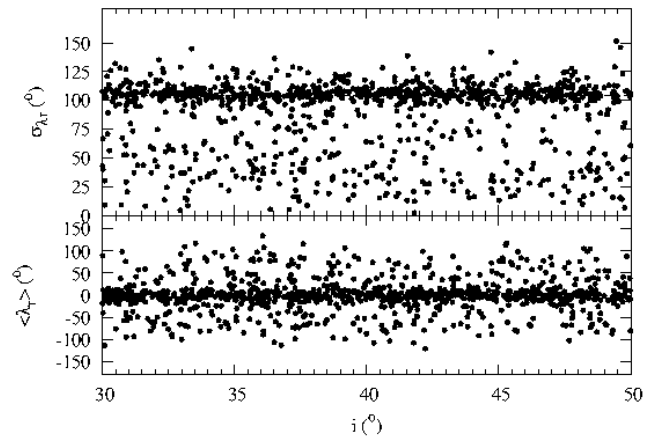


**Figure 8.** Same as Fig. 6 but for the initial value of the inclination.

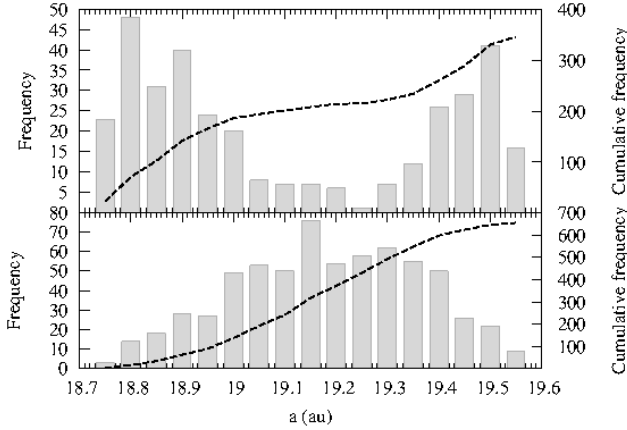


**Figure 9.** Distribution in initial semimajor axis for objects with standard deviation of the resonant angle,  $\sigma_{Lr}$ , in the range  $100^\circ$ – $108^\circ$  (likely passing orbits, top panel) and outside that range (bottom panel). Out of  $10^3$  orbits studied, 346 have  $\sigma_{Lr} \in (100^\circ, 108^\circ)$ .

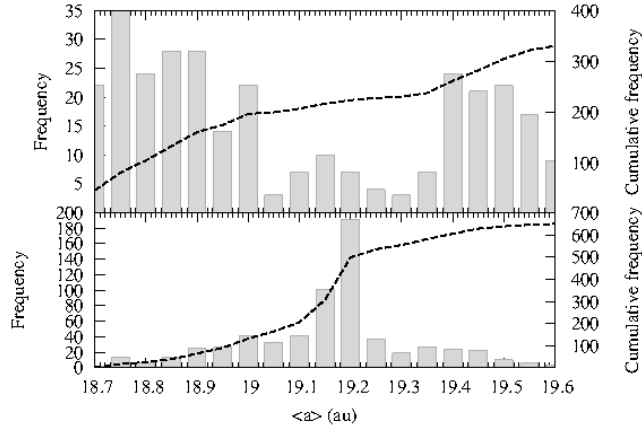


**Figure 10.** Same as Fig. 9 but for the average value of the semimajor axis.

shows that the co-orbital region approximately goes from 19.0 to 19.4 au. Outside that range in semimajor axis, most trajectories become passing orbits. However, even deep inside Uranus’ co-orbital zone not all the values of the semimajor axis are equally favourable regarding stability. Figure 10 shows the distribution for the average value of the semimajor axis. The extension of the co-orbital zone is confirmed, but those orbits with values of the osculating semimajor axis in the range 19.1–19.2 au are far more stable.

Although the previous analysis strongly suggests that 2015 DB<sub>216</sub> is not a statistical accident and that more temporary Uranian co-orbitals must exist at high orbital inclinations, our relatively short and non-extensive integrations appear to leave the question of long-term stability open. Can we expect that objects moving in high-inclination orbits like that of 2015 DB<sub>216</sub> will spend 10 or 100 Myr trapped in the 1:1 mean motion resonance with Uranus? Figs 11 and 12 suggest an answer in the affirmative. In order to study the variation over time of a given orbital parameter, we have computed the absolute value of the difference between the initial and final values of the parameter and divided by the integrated time. Figure 11 shows these drifts in  $a$ ,  $e$  and  $i$  per Myr. It is obvious that, taking into account the span of the co-orbital zone, relatively long-term stability is possible.

Figure 12 shows the average values of  $a$  and  $e$  as a function

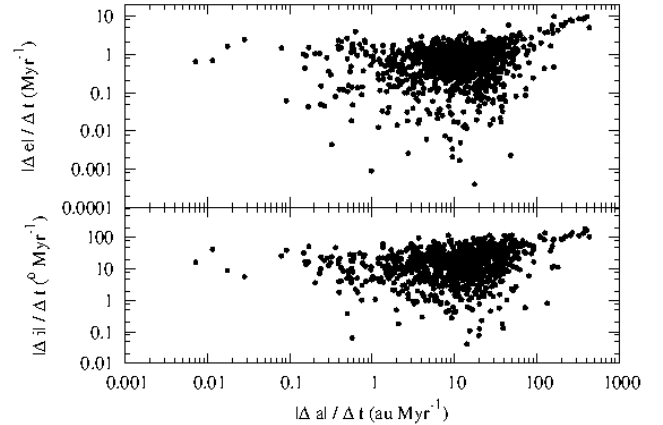


**Figure 11.** Variation of the eccentricity (top panel) and the inclination (bottom panel) over time as a function of the corresponding variation in semimajor axis (see the text for details).

of the drift in  $a$ . From there, the most stable test orbits are found for the ranges in  $\langle a \rangle$  and  $\langle e \rangle$  of 19.0–19.6 au and 0.15–0.35, respectively. The range in  $\langle a \rangle$  appears to be somewhat in conflict with the values found above, but there is an additional type of co-orbital motion that does not require libration of the resonant angle: minor bodies following passing orbits with small Jacobi constants but still moving in unison with a host planet as described by Namouni (1999). This orbital regime is also known as the Kozai domain because it corresponds to a Kozai resonance (Kozai 1962). Under the Kozai resonance, both eccentricity and inclination oscillate with the same frequency but out of phase; when the value of the eccentricity reaches its maximum the value of the inclination is the lowest and vice versa ( $\sqrt{1-e^2} \cos i \sim \text{constant}$ ); therefore, relatively large oscillations in  $e$  and  $i$  are still compatible with long-term stability in this case. The most stable test orbit generated in our exploratory calculations could remain virtually unchanged for time-scales well in excess of 10 Myr (see Fig. 12) and it is not a classical (librating) co-orbital but a fictitious object in the Kozai domain. The actual values of the semimajor axis, 19.2 au, and eccentricity, 0.32, of 2015 DB<sub>216</sub> place this object in the most stable region of the orbital domain probed in Fig. 12. If such orbits represent nearly 0.3 per cent of the ones explored in this section and one actual object has already been found, 2015 DB<sub>216</sub>, a significant number of less stable high-inclination, recurring Uranian co-orbitals are likely to exist.

## 7 CONCLUSIONS

In this paper, we have analysed the orbital behaviour of 2015 DB<sub>216</sub> that is the fourth known minor body to be trapped in a 1:1 mean motion resonance with Uranus. Our numerical integrations show that it currently moves in a complex, horseshoe-like orbit when viewed in a frame of reference corotating with Uranus. The object exhibits resonance angle nodding as it undergoes recurrent co-orbital episodes with Uranus. Its high orbital inclination clearly separates this object from the other three known Uranian co-orbitals and makes it more stable. Its discovery circumstances also single this minor body out among objects currently trapped into the 1:1 commensurability with Uranus, hinting at the presence of a large number of similar objects. If they are inherently more stable at higher inclinations, that should have an impact on the population of Ura-

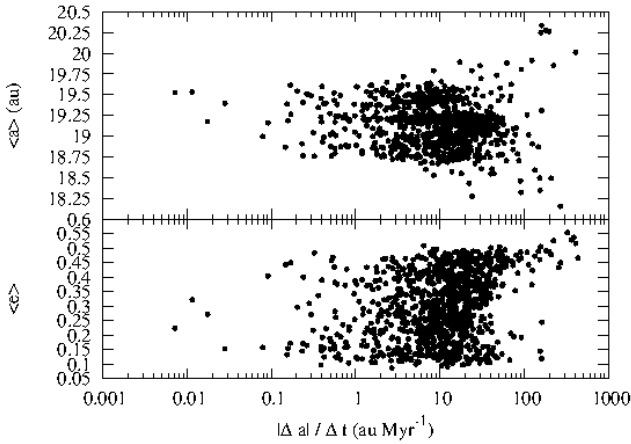


**Figure 12.** Average value of the semimajor axis (top panel) and the eccentricity (bottom panel) as a function of the variation of the semimajor axis over time.

nian irregular moons. All but one are retrograde and their orbital inclinations are in the range  $139^{\circ}$ – $167^{\circ}$  or in prograde terms  $41^{\circ}$ – $13^{\circ}$ . Five irregular moons out of 9 have inclinations in the range  $139^{\circ}$ – $147^{\circ}$ . As for the mechanism responsible for the activation of the co-orbital states, multibody mean motion resonances trigger the transitions as previously observed for other Uranian co-orbitals.

**ACKNOWLEDGEMENTS**

We thank the anonymous referee for his/her constructive and helpful report, and S. J. Aarseth for providing the code used in this research. In preparation of this paper, we made use of the NASA Astrophysics Data System, the ASTRO-PH e-print server, and the MPC data server.

**REFERENCES**

Aarseth S. J., 2003, *Gravitational N-body simulations*. Cambridge Univ. Press, Cambridge, p. 27  
 Alexandersen M., Gladman B., Greenstreet S., Kavelaars J. J., Petit J.-M., Gwyn S., 2013, *Science*, 341, 994  
 Avdyushev V. A., Banschikova M. A., 2007, *Sol. Syst. Res.*, 41, 413  
 Beaugé C., Ferraz-Mello S., Michtchenko T. A., 2003, *ApJ*, 593, 1124  
 Bordovitsyna T., Avdyushev V., Chernitsov A., 2001, *Celest. Mech. Dyn. Astron.*, 80, 227  
 de la Fuente Marcos C., de la Fuente Marcos R., 2012, *MNRAS*, 427, 728  
 de la Fuente Marcos C., de la Fuente Marcos R., 2013, *A&A*, 551, A114  
 de la Fuente Marcos C., de la Fuente Marcos R., 2014, *MNRAS*, 441, 2280  
 Dvorak R., Bzszó Á., Zhou L.-Y., 2010, *Celest. Mech. Dyn. Astron.*, 107, 51  
 Gallardo T., 2006, *Icarus*, 184, 29  
 Gallardo T., 2014, *Icarus*, 231, 273  
 Giorgini J. D. et al., 1996, *BAAS*, 28, 1158  
 Granvik M., Vaubaillon J., Jedicke R., 2012, *Icarus*, 218, 262  
 Grav T., Holman M. J., Gladman B. J., Aksnes K., 2003, *Icarus*, 166, 33  
 Henon M., 1969, *A&A*, 1, 223  
 Holman M. J., Wisdom J., 1993, *AJ*, 105, 1987  
 Ito T., Tanikawa K., 2002, *MNRAS*, 336, 483  
 Jackson J., 1913, *MNRAS*, 74, 62  
 Ketchum J. A., Adams F. C., Bloch A. M., 2013, *ApJ*, 762, 71  
 Kortenkamp S. J., 2005, *Icarus*, 175, 409  
 Kozai Y., 1962, *AJ*, 67, 591  
 Kwiatkowski T. et al., 2009, *A&A*, 495, 967

Lee M. H., Peale S. J., 2002, *ApJ*, 567, 596  
 Makino J., 1991, *ApJ*, 369, 200  
 Marzari F., Tricarico P., Scholl H., 2003, *A&A*, 410, 725  
 Murray C. D., Dermott S. F., 1999, *Solar System Dynamics*, Cambridge Univ. Press, Cambridge, p. 97  
 Namouni F., 1999, *Icarus*, 137, 293  
 Nesvorný D., Dones L., 2002, *Icarus*, 160, 271  
 Nesvorný D., Alvarellos J. L. A., Dones L., Levison H. F., 2003, *AJ*, 126, 398  
 Press W. H., Teukolsky S. A., Vetterling W. T., Flannery B. P., 2007, *Numerical Recipes: The Art of Scientific Computing*, 3rd edn. Cambridge Univ. Press, Cambridge  
 Sheppard S. S., Jewitt D., Kleyna J., 2005, *AJ*, 129, 518  
 Sitarski G., 1998, *Acta Astron.*, 48, 547  
 Sitarski G., 1999, *Acta Astron.*, 49, 421  
 Sitarski G., 2006, *Acta Astron.*, 56, 283  
 Standish E. M., 1998, *JPL Planetary and Lunar Ephemerides, DE405/LE405*, Interoffice Memo. 312.F-98-048, Jet Propulsion Laboratory, Pasadena, CA  
 Tanikawa K., Ito T., 2007, *PASJ*, 59, 989

This paper has been typeset from a  $\text{\TeX}/\text{\LaTeX}$  file prepared by the author.